Available online at www.sciencedirect.com
SCIENCE DIRECT®
Fluid Dynamics Research 38 (2006) 660–681
FLUID DYNAMICS RESEARCH

Direct numerical simulations of gas/liquid multiphase flows

Gretar Tryggvason*, Asghar Esmaeeli, Jiacai Lu, Souvik Biswas

Worcester Polytechnic Institute, 100 Institute Road, Worcester, MA 01609, USA

Received 29 June 2004; received in revised form 27 July 2005; accepted 2 August 2005

Communicated by K. Ishii

Abstract

Direct numerical simulations of bubbly flows are reviewed and recent progress is discussed. Simulations, of homogeneous bubble distribution in fully periodic domains at relatively low Reynolds numbers have already yielded considerable insight into the dynamics of such flows. Many aspects of the evolution converge rapidly with the size of the systems and results for the rise velocity, the velocity fluctuations, as well as the average relative orientation of bubble pairs have been obtained. The challenge now is to examine bubbles at higher Reynolds numbers, bubbles in channels and confined geometry, and bubble interactions with turbulent flows. We briefly review numerical methods used for direct numerical simulations of multiphase flows, with a particular emphasis on methods that use the so-called "one-field" formulation of the governing equations, and then discuss studies of bubbles in periodic domains, along with recent work on wobbly bubbles, bubbles in laminar and turbulent channel flows, and bubble formation in boiling.
© 2006 The Japan Society of Fluid Mechanics and Elsevier B.V. All rights reserved.

Keywords: Direct numerical simulations; Gas/liquid flows; Bubbly flows; Front tracking; Multiphase flows

1. Introduction

Gas/liquid multiphase flows occur in a wide range of natural and man-made situations. Examples include boiling heat transfer, cloud cavitation, bubble columns and reactors in the chemical industry, cooling circuits of power plants, spraying of liquid fuel and paint, emulsions, rain, bubbles and drops due

* Corresponding author. Fax: +1 508 831 5680.
E-mail address: gretar@wpi.edu (G. Tryggvason).

0169-5983/$30.00 © 2006 The Japan Society of Fluid Mechanics and Elsevier B.V. All rights reserved.
doi:10.1016/j.fluiddyn.2005.08.006

to wave breaking in the oceans, and explosive volcanic eruptions. Understanding the flow of gas/liquid flows is therefore of major technological as well as scientific interest.

Although the fundamental equations governing the behavior of gas and liquids, as well as the conditions at a fluid interface are reasonably well known, in most practical applications it is necessary to deal with systems where the ratio between the size of the system and the smallest continuum scale is many orders of magnitude. For such systems it is not practical to resolve the continuum scales and predictions must be made using equations that describe the average behavior of the system. Equations for the averaged flow can take several different forms, but the two-fluid model, where separate equations are solved for the dispersed and the continuous phase, is the most common approach. For details of two-fluid modeling see Drew (1983), Ishii (1987), Drew and Lahey (1993), and Zhang and Prosperetti (1994). The situation is similar to turbulence in homogeneous fluids, except that the small-scale motion is more complex. Since no attempt is made to resolve the unsteady motion of individual particle, closure relations are necessary for the unresolved motion and the forces between the particle and the continuous phase. Closure relations have traditionally been determined through a combination of dimensional arguments and correlation of experimental data but direct numerical simulations (DNS), where the unsteady Navier–Stokes equations are solved on fine enough grids to fully resolve all flow scales, have played an increasingly important role in the development of closure models for turbulence in homogeneous fluids. While DNS of multiphase flows have lagged significantly behind homogeneous flows, considerable progress has been made recently, particularly for bubbly flows. The goal of DNS of multiphase flows is both to generate insight and understanding of the basic behavior of multiphase flow—such as the forces on a single bubble or a drop, how bubbles and drops affect the flow, and how many bubbles and drops interact in dense disperse flows—as well as to provide data for the generation of closure models for engineering simulations of the averaged flow field. As in turbulent flow of a single-phase fluid, multiphase flows generally possess a large range of scales, ranging from the sub-millimeter size of a bubble or an eddy to the size of the system under investigation. Multiphase flows, like single-phase turbulent flows, exhibit a great deal of universality and it is almost certain that re-computing small-scale behavior that is already understood is not necessary. DNS should be able to provide both the insight and the data for the modeling at the smallest scales.

In this review we will focus on dispersed bubbly flows. That is not to imply that such flows are the only one of interest. Stratified flows where there is a well-defined free surface, or sprays where drops are moving through air, are also important and have been the subject of several numerical investigations. The vastness of the subject does, however, require us to limit the scope of the discussion, and as considerable progress has been made recently in understanding bubbly flows, it is natural to focus on such flows.

DNS of bubbly flows, where the flow around each bubble is fully resolved and viscosity, inertia, and surface tension are fully accounted for, have already been used to study the behavior of systems containing up to O(100) bubbles. These simulations have already yielded large amount of new insight into the dynamics of bubbly flows, including the identification of preferred relative orientation of bubble pairs, and data for the bubble induced flow. DNS have also been used to explain the importance of deformability, both for the motion of a single bubble in a shear flow as well as the collective dynamics of many bubbles. Most of the work done so far has, however, been for bubbles in periodic domains with relatively modest rise Reynolds numbers. While such systems are of relevance for high viscosity liquids, it is obviously important to understand what happens as the Reynolds number increases and how walls and pre-existing turbulence interact with the bubbles.

2. Numerical methods

Before we discuss results of DNS of bubbly flows, we will briefly review numerical methods used for direct numerical simulations of multiphase flows. Most success has been achieved using methods based on the so-called "one-field" formulation of the governing equations and we will discuss this formulation in the next section.

Although the need for DNS to help with the construction of reliable closure models has been recognized for a long time, it is only recently that major progress has been made, particularly for finite Reynolds number flows where the full Navier–Stokes equations must be solved. Simplified models—where inertia is completely ignored (Stokes flow) or viscous effects are ignored (inviscid, potential flows)—were, however, used earlier by several investigators. If the bubbles can be assumed to be undeformable spheres, the results are particularly simple since in both the Stokes and the potential flow limit it is possible to reduce the governing equations to a system of coupled ordinary differential equations for the particle positions. See Brady and Bossis (1988) for a review of early work on Stokes flow and Sangani and Didwania (1993) and Smereka (1993) for inviscid flows.

For both Stokes flows and potential flows, the motion of deformable boundaries can be simulated with boundary integral techniques. One of the earliest papers to use boundary integral method for inviscid flows was Longuet-Higgins and Cokelet (1976) who examined breaking waves. This paper was enormously influential and was followed by a large number of very successful extensions and applications, particularly for water waves (Baker et al., 1982; Vinje and Brevig, 1981; Schultz et al., 1994; and others). Other applications include the evolution of the Rayleigh–Taylor instability (Baker et al., 1980), the growth and collapse of cavitation bubbles (Blake and Gibson, 1981; Robinson et al., 2001), the generation of bubbles and drops due to the coalescence of bubbles with a free surface (Oguz and Prosperetti, 1990; Boulton-Stone and Blake, 1993), the formation of bubbles and drops from an orifice (Oguz and Prosperetti, 1993), and the interactions of vortical flows with a free surface (Yu and Tryggvason, 1990), just to name a few. For a review of recent progress see Hou et al. (2001). Fully three-dimensional computations include Chahine and Duraiswami (1992) who computed the interactions of a few inviscid cavitation bubbles and Xue et al. (2001) who have simulated a three-dimensional breaking wave.

The use of boundary integral simulations for unsteady two-fluid Stokes problems started with Youngren and Acrivos (1976) and Rallison and Acrivos (1978) who simulated the deformation of a bubble and a drop, respectively, in an extensional flow. Pozrikidis and collaborators later examined several aspects of the suspension of drops, starting with a study by Zhou and Pozrikidis (1993) of the suspension of a few two-dimensional drops in a channel. Simulations of fully three-dimensional suspensions have been done by Loewenberg and Hinch (1996) and Zinchenko and Davis (2000). The method has been described in detail in the book by Pozrikidis (1992), and Pozrikidis (2001) gives a very complete summary of the various applications.

For flows where the bubbles can be assumed to be much smaller than any flow structure, several authors have used the so-called point particle approximation. In this approach the fluid particles are assumed to be so small that they can be approximated by a single point and the fluid motion computed by solving the Navier–Stokes equations for homogeneous fluid. The particles are moved by integrating an equation of motion where the forces on the particle are related to the fluid motion interpolated at the location of the particle. In one-way coupling the effect of the particle on the fluid is ignored, but in two-way coupling a force equal but opposite to the total force on the particle is added to the momentum equations for the fluid. In the limit of zero Reynolds number the forces on the particles can be computed analytically, but at higher

Reynolds numbers it is necessary to use empirical relations. For a recent review see Michaelides (2003). Even in two-way coupling the flow around each particles is not completely resolved and particles do not "see" each other. Recently, however, Pan and Banerjee (1997) and Xu et al. (2000) have introduced methods where the particle is spread over a few grid points and the effect of the particle on the fluid and the interactions between particles are partially accounted for. It seems likely that between the full resolution of each bubble and the point particle approximation there exist a continuum of models that account for the presence of the bubbles to a different degree of accuracy and that require different level of empirical input.

Attempts to simulate multiphase flows for intermediate Reynolds numbers are essentially as old as computational fluid dynamics for homogeneous flows. The Marker-And-Cell (MAC) method developed at Los Alamos by Harlow and collaborators was originally intended for fluid with a free surface (Harlow and Welch, 1965). Two sample computations of the so-called dam breaking problem were included and Harlow and Welch (1966) examined the Rayleigh–Taylor problem. The method was extended to two-fluid problems by Daly (1969a) who computed the evolution of the Rayleigh–Taylor instability for finite density ratios and Daly and Pracht (1968) who examined the initial motion of density currents. Surface tension was then added by Daly (1969b) and the method again used to examine the Rayleigh–Taylor instability. Other papers, where other authors used the MAC method, followed: Chan and Street (1970) applied it to free surface waves, Foote (1973, 1975) simulated the oscillations of an axisymmetric drop and the collision of a drop with a rigid wall, and Chapman and Plesset (1972) and Mitchell and Hammitt (1973) simulated the collapse of a cavitation bubble.

Although the MAC method was capable of producing results that can only be described as way ahead of the times, the markers could result in surface irregularities and deteriorated surface quality. The markers were therefore replaced by a marker function in the Volume-Of-Fluid (VOF) method discussed by Hirt and Nichols (1981). The VOF method has since been extended in various ways by a number of authors. For a review of VOF methods, see Scardovelli and Zaleski (1999). Other methods, based on similar ideas but advecting the marker function in a different way include the level set method (reviewed by Osher and Fedkiw, 2001; Sethian, 2001) and the CIP method of Yabe and collaborators (see Yabe et al., 2001, for a review).

The MAC methodology and its successors are all based on using regular stationary grids and working with one set of governing equations for the whole flow field, irrespectively of what fluid occupies a particular grid point. We will discuss this approach in more detail in the next section. Other approaches are, of course, possible and several authors have developed methodologies based on grids that are aligned with the fluid interface at any given time. One of the earliest contribution was by Hirt et al. (1970) who used structured boundary fitted Lagrangian grids. This approach is particularly well-suited when the interface topology is relatively simple and no unexpected interface configurations develop. Sometimes only the grid line on the interface is moved with the fluid and the grid away from the interface is generated using standard grid generation techniques. This was the approach taken by Ryskin and Leal (1984), who computed the steady rise of a buoyant, deformable, axisymmetric bubble. Several authors have used this approach to examine relatively simple problems but fully three-dimensional simulations are relatively rare (see, however, Takagi et al., 1997, for one example) and it is unlikely that body fitted structured grids will be the method of choice for very complex problems such as the three-dimensional unsteady motion of several particles. Unstructured grids, on the other hand, offer much more flexibility, and as numerical methods for unstructured grids continue to be developed, the use of unstructured grids that move with a fluid interface becomes an increasingly attractive approach.

A large number of methods that fall into this general category have been developed by a number of investigators. Those include Oran and Boris (1987) who simulated the breakup of a two-dimensional drop; Shopov et al. (1990) who examined the initial deformation of a buoyant bubble; and Fukai et al. (1995) who did axisymmetric computations of the collision of a single drop with a wall, just to name a few.

While both interface capturing methods, where each fluid is identified by a marker function, and methods based on using separate moving grids in each fluid have been used for a wide variety of problems, several investigators have sought methods that are more accurate than the former, yet simpler than the latter. Front tracking, where the interface is marked by connected marker points but a fixed grid is used for the fluid within each phase, has been particularly successful. In the method of Tryggvason and collaborators (Unverdi and Tryggvason, 1992a,b; Tryggvason et al., 2001) the tracked front is used to advect a smoothed marker function and to compute the surface tension. The method is therefore very similar to methods that work directly with a grid-marker function, but the advection of the interface is greatly improved. Other methods have been designed to capture the interface more accurately. These include the method of Glimm and collaborators (Glimm and McBryan, 1985), where the fixed grid is modified near the front to make a grid line follow the interface, as well as more recent "sharp-interface methods" (such as Fedkiw et al., 1999; Ye et al., 1999; Lee and LeVeque, 2003). We will discuss the method of Tryggvason in more detail in the next section.

In addition to methods designed to handle deformable bubbles, numerical techniques have also been designed to follow the unsteady motion and interaction of rigid particles. These methods have been based on moving unstructured grids (see Hu et al., 2001; Johnson and Tezduyar, 1997, for reviews) and the "fictitious domain approach" (Glowinski et al., 2001). While the phase boundary is not deformable in the usual sense, it certainly moves as the particles move.

In addition to methods based on standard discretizations of the Navier–Stokes equations, several lattice Boltzmann methods have recently been developed for simulations of finite Reynolds number multiphase flows. For a discussion see, for example, Shan and Chen (1993) and Sankaranarayanan et al. (2002).

For reviews of computational methods for multiphase flows, see Hyman (1984) and Floryan and Rasmussen (1989) for a general discussion; Scardovelli and Zaleski (1999) for VOF methods; Anderson et al. (1998) for phase field methods; and the book by Shyy et al. (1996). Various articles about methods for computations of multiphase systems and related problems can be found in a special issue of the Journal of Computational Physics (volume 169, 2001).

3. One-fluid approach

The oldest as well as the most successful approach to simulations of multifluid flows is to use one set of equations for the entire computational domain. To include the interface boundary conditions, interface effects must be added as singular terms. The Navier–Stokes, with the singular surface tension term added, are

$$\frac{\partial \mathbf{u}}{\partial t} + \nabla \cdot \mathbf{u}\mathbf{u} = -\frac{1}{\rho}\nabla P + \mathbf{f} + \frac{1}{\rho}\nabla \cdot \mu(\nabla \mathbf{u} + \nabla^{\mathrm{T}}\mathbf{u}) + \frac{1}{\rho}\sigma\kappa\delta(n)\mathbf{n}. \tag{1}$$

This equation is valid for the whole flow field, even when the density field ρ and the viscosity field μ, change discontinuously. Here $\mathbf{u}$ is the velocity, P is the pressure, and $\mathbf{f}$ is a body force. Surface forces are

added at the interface and $\delta(n)$ is a one-dimensional delta-function of the normal coordinate n. κ is the curvature for two-dimensional flows and twice the mean curvature for three-dimensional flows, σ is the surface tension, and $\mathbf{n}$ is a unit vector normal to the interface.

Mass conservation is given by

$$\frac{\partial \rho}{\partial t} + \nabla \cdot \rho \mathbf{u} = 0. \tag{2}$$

If the fluids are incompressible, then the density of a fluid particle remains constant, i.e.

$$\frac{D\rho}{Dt} = 0, \tag{3}$$

which reduces the mass conservation (2) to

$$\nabla \cdot \mathbf{u} = 0. \tag{4}$$

Usually the viscosity in each fluid is also taken to be constant, so

$$\frac{D\mu}{Dt} = 0. \tag{5}$$

The "one-fluid" equations are an exact rewrite of the Navier–Stokes equations and a simple integration over a "pill-box" containing the interface allows us to recover the usual interface conditions.

The Navier–Stokes equations, as written above, can in principle be solved by any method suitable for constant density fluids and generally a projection methods is used to advance the solution in time. In a projection method a preliminary velocity field is first computed based on the advection and diffusion terms, plus body forces and the singular interface force for multiphase flows. The preliminary velocity is in general not divergence free and this velocity is therefore corrected (or projected onto the space of divergence free velocities—hence the name) by adding the pressure gradient needed to ensure zero divergence. The equation for the pressure is obtained by taking the (numerical) divergence of the momentum equation and setting the divergence of the new velocity field to zero. Although the approach for multifluid flow parallels what is done for single-phase flow, in practice there are three complications. First of all, and common to essentially all methods based on the one-fluid formulation, is that the pressure equation is not separable as for single-phase flow and is therefore more difficult to solve, particularly for large density differences. The second and third difficulties are the accurate advection of material fields (Eqs. (3) and (5)), and the computation of the surface tension. Generally, Eqs. (3) and (5) are not solved directly but a marker function f that identifies the different fluids is used. The marker function is defined by $f = 1$ in one fluid and $f = 0$ in the other and the material properties are determined according to the value of the marker function. The various ways that the marker function is advected distinguishes between the different methods used for the numerical implementation of the one-fluid formulation.

Since the marker function moves with the fluid, its motion is governed by

$$\frac{Df}{Dt} = \frac{\partial f}{\partial t} + \mathbf{u} \cdot \nabla f = 0. \tag{6}$$

This equation can, of course, be solved by any method suitable for hyperbolic equations, but—as for the advection of a discontinuity in general—low order linear schemes smear the interface and higher order linear schemes generate oscillations around the interface. Modern nonlinear schemes for shock capturing (see LeVeque, 2002, for example) do a reasonable job for a short time but since there is no mechanism to sharpen an interface that has deteriorated (unlike shocks which are "self-sharpening") it is difficult to keep the shocks sharp for all times. Furthermore, since the marker function generally is constant within each fluid, it seems self-evident that it should be possible to take advance of this simplification to construct schemes that preserve the interface for all times. In the VOF method the interface is advected by using the value of f in interface cells to "reconstruct" the exact location of the interface. In one dimension the interface location makes it possible to compute exactly the flux of f from one cell to the next. The extension to two- and three-dimensions has, however, turned out to be challenging. Early implementations were based on treating each direction independently as one-dimensional problems, but this resulted in a jagged interface with considerable amount of "floatsma" and "jetsam." In later implementations the "reconstruction" has been done using linear (or higher order) fits in each cell, greatly improving the quality of the solution but also making the method much more complex. In the CIP method (see Yabe et al., 2001, for a recent reference) the interface profile is reconstructed by fitting a high-order polynomial to the function and its derivatives, which are advected separately. While the VOF and the CIP method attempt to keep the interface as sharp as possible, in the level set method a smooth function is advected by standard advection methods and the interface is identified by the zero contour (the level set). Since the material fields have to be reconstructed from the level set function, it is, however, necessary to modify the advection to keep the shape of the function away from the interface unchanged. This is usually done by forcing the marker function to represent the shortest distance to the interface (Sussman et al., 1994). In all the methods listed here, the curvature of the interface (for computations of surface tension) is found by differentiating the gradient of the marker function.

In the front tracking method of Unverdi and Tryggvason (1992a,b) the fluid interface is identified by connected marker points that form an unstructured mesh, usually referred to as the front. The surface tension, as well as the gradients of the density and viscosity are singular delta-functions but to transfer the front singularities to the fixed grid, the delta functions are approximated by smoother functions with a compact support on the fixed grid. The front points are advected with the fluid velocity and at each time step the density and the viscosity fields are reconstructed from the new front location by integrating the smooth grid-delta function. For a given smoothing function, the thickness of the interface is directly related to the grid size and while a very coarse grid may lead to a poor approximation of the discontinuous density field, refining the grid produces a sharper transition zone as demonstrated in Fig. 1. The bubbles in the top frame are resolved by only about 10 grid points per diameter but in the bottom frame the resolution has been doubled. Since the boundary between the fluids (the front) usually undergoes considerable deformation during the phase change, it is necessary to modify the surface mesh dynamically during the course of the computations. The surface mesh consists of points that are linked by elements and both the points and the elements are arranged in a linked list so it is relatively easy to change the structure of the front, including adding and deleting points and elements. For details of the implementation, see Tryggvason et al. (2001). Fig. 2, which shows the velocity field, computed on a fixed mesh, around a bubble represented by triangular elements summarizes the computational approach.

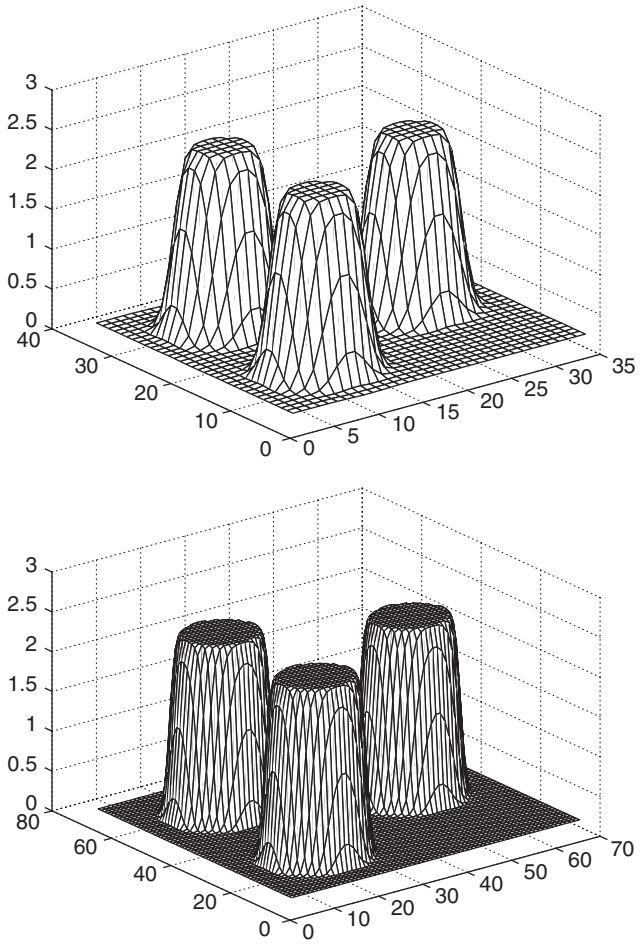

Fig. 1. Two frames showing an indicator function for three bubbles. The bubbles in the top frame, computed using a 32^2 grid, are resolved by only about 10 grid points per diameter but in the bottom frame the resolution is doubled.

4. Homogeneous bubbly flows

Homogeneous bubbly flows, where many buoyant bubbles rise together in an initially quiescent fluid, are perhaps one of the simplest example of a disperse multiphase flow. Such flows can be simulated using periodic domains where the bubbles in each period interact freely, but the configuration is repeated infinitely many times in each coordinate direction. As the number of bubbles in each period is increased the bubbles generally rise unsteadily, repeatedly undergoing close interactions with other bubbles. The behavior is, however, statistically steady and the average motion (averaged over long enough time) does not change. Once the size of the system is large enough, information obtained by averaging over each period should be representative of a truly homogeneous bubbly flow.

In the limit of small bubbles and dilute flows the point particle approximation has been used by several authors to examine the effect of bubbles on turbulent flows (see, Spelt and Biesheuvel, 1997; Druzhinin

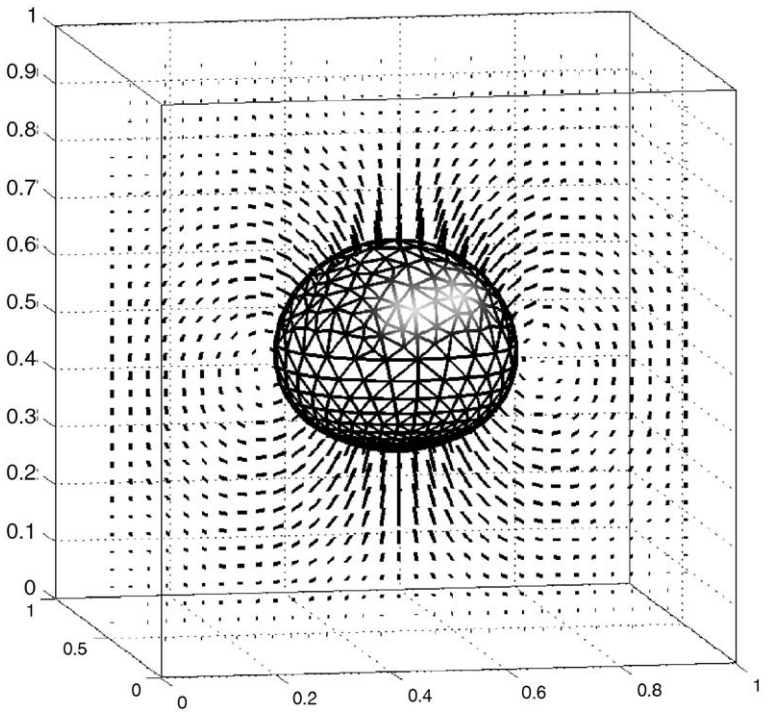

Fig. 2. Simulation of a single bubble using the front-tracking method of Tryggvason and collaborators. The bubble surface is represented by a triangular grid but the velocity field is computed on a regular fixed mesh.

and Elghobashi, 2001, for example). This approximation, however, imposes severe limitations on the size of the bubbles and how accurately bubble interactions are accounted for. In many practical situations—air bubbles in water, for example—the effect of viscosity is relatively small and it seems plausible that inviscid models can capture the dynamics. Using the inviscid potential flow approximation, Sangani and Didwania (1993) and Smereka (1993) observed, however, that spherical bubbles in a periodic box tended to form horizontal "rafts," particularly when the variance of the bubble velocities was small. As this rafting is generally not observed experimentally, the results cast considerable doubt on the utility of the potential flow approximation for the interactions of many bubbles. This is somewhat unexpected since for a single bubble this approximation is excellent (see, however, Harper, 1997, for a discussion of bubbles rising in-line). While transient interactions of a few deformable bubbles have been examined using boundary integral methods, no simulations of the long-time evolution of many deformable bubbles have been done, and given the failure of the potential flow approximation for rigid bubbles at high Reynolds numbers, it seems unlikely that such studies would be applicable to realistic situations.

To fully account for the effects of viscosity, inertia, and bubble interactions at intermediate Reynolds numbers it is necessary to solve the full unsteady Navier–Stokes equations. Simulations of a single bubble go back to the papers of Ryskin and Leal (1984) but studies of the unsteady interactions of two or more bubbles are more recent. Unverdi and Tryggvason (1992a,b) computed the interactions of two, two- and three-dimensional bubbles, Esmaeeli and Tryggvason (1996) followed the evolution of a few hundred two-dimensional bubbles and Esmaeeli and Tryggvason (1998, 1999) simulated the unsteady motion of

several two- and three- dimensional bubbles. More recently, Bunner and Tryggvason (1999, 2002a,b, 2003) examined three-dimensional systems with a much larger number of bubbles. We will review the simulations of Esmaeeli and Tryggvason (1998, 1999) and Bunner and Tryggvason (1999, 2002a,b, 2003) in more detail below. Other studies of the motion and interactions of many bubbles have been done by several Japanese authors. Early work, using the VOF method to compute the motion of a single two-dimensional bubble can be found in Tomiyama et al. (1993) and more recent work on bubble interactions, using both VOF and the lattice Boltzmann Method, is presented in Takada et al. (2000, 2001).

Major progress has also been made in the simulation of finite Reynolds number suspension of rigid particles. Feng et al. (1994, 1995) simulated the two-dimensional, unsteady motion of one and two rigid particles, Hu (1996) computed the motion of a few hundred two-dimensional particles and fully three-dimensional simulations of 100 particles were presented by Johnson and Tezduyar (1997). Recent papers include simulations of over 1000 spheres by Pan et al. (2002) and a study of the fluidization of 300 circular particles in plane Poiseuille flow by Choi and Joseph (2001). There are, of course, some differences between the behavior of deformable bubbles and solid particles, but the development of DNS for particle suspensions has generally paralleled the development for bubbly flows.

The simulations of Tryggvason and coworkers have now added considerably to our understanding of bubbly flows at moderate Reynolds numbers. Esmaeeli and Tryggvason (1998) examined a case where the average rise Reynolds number of the bubbles remained relatively small (i.e. 1–2) and Esmaeeli and Tryggvason (1999) looked at another case where the Reynolds number was 20–30, depending on the void fraction. In both cases, most of the simulations were limited to two-dimensional flows, although a few three-dimensional simulations with up to eight bubbles were included. Simulations of freely evolving arrays were compared with regular arrays and it was found that while freely evolving bubbles at low Reynolds numbers rise faster than a regular array (in agreement with Stokes flow results), at higher Reynolds numbers the trend was reversed and the freely moving bubbles rose slower. The time averages of the two-dimensional simulations were generally well converged but exhibited a dependency on the size of the system. This dependency was stronger for the low Reynolds number case than the moderate Reynolds number one. Although many of the qualitative aspects of the interactions of a few three-dimensional bubbles are captured by two-dimensional simulations, the much stronger interactions between two-dimensional bubbles can lead to quantitative differences. The rise velocity at low Reynolds number was reasonably well predicted by Stokes flow based models. The bubble interaction mechanism was, however, quite different. At finite Reynolds numbers, two-bubble interactions take place by the drafting, kissing, and tumbling mechanism of Fortes et al. (1987), where a bubble is drawn into the wake of a bubble in front. Once in the wake the bubble is shielded from the oncoming flow, it accelerates and catches up with the bubble in front ("drafting"). After colliding ("kissing"), the bubbles tumble and drift apart. This behavior is, of course, very different from either a Stokes flow where two bubbles do not change their relative orientation unless acted on by a third bubble, or potential flow where a bubble is pushed away from the bubble in front, not drawn into its wake.

Bunner and Tryggvason (2002a,b) simulated a much larger number of nearly spherical three-dimensional bubbles using a parallel version of the method used by Esmaeeli and Tryggvason (1998, 1999). Their largest simulation followed the motion of 216 three-dimensional buoyant bubbles in a periodic domain for a relatively long time. The governing parameters were selected such that the average rise Reynolds number was about 20–30 (close to Esmaeeli and Tryggvason, 1999, but not the same), depending on the void fraction. The simulations were carried out for a long enough time so the average behavior of the system was well defined, as in the two-dimensional simulations of Esmaeeli and Tryggvason (1998,

1999). Simulations with different number of bubbles were used to explore the dependency of the various average quantities on the size of the system. The average rise Reynolds number and the Reynolds stresses were essentially fully converged for systems with 12 bubbles, but the average fluctuations of the bubble velocities required larger systems. Examination of the pair distribution function for the bubbles showed a preference for horizontal alignment of bubble pairs, independent of system size, but the distribution of bubbles remained nearly uniform. The results showed that there is an increased tendency for the bubbles to line up side-by-side as the rise Reynolds number increases, suggesting a monotonic trend from the essentially random orientations found by Ladd (1993) for Stokes flow, toward the strong layer formation seen in the potential flow simulations of Sangani and Didwania (1993) and Smereka (1993). The simulations of Bunner and Tryggvason (2002b) also showed that while the Reynolds stress tensor scaled in a way predicted by potential flow cell models, and while the horizontal velocity fluctuations were comparable in magnitude, the vertical velocity fluctuations were considerably higher. The implication of these results for the modeling of velocity fluctuations due to the motion of the bubbles in simulations of the averaged properties is, however, not completely clear at this time. It may well be that using potential flow models for the pseudoturbulence generated by the passing of a bubble is still the most appropriate approach, and the effect of turbulence generated by the bubble wake (due to deposition of vorticity) would be best taken into account by using a turbulence model, even when the flow due to a single bubble is laminar.

To examine the effect of bubble deformation, Bunner and Tryggvason (2003) conducted two sets of simulations using 27 bubbles per periodic domain. In one case the bubbles were spherical, in the other the bubbles deformed into ellipsoids. The nearly spherical bubbles quickly reached a well-defined average rise velocity and remained nearly uniformly distributed in the computational domain. The deformable bubbles initially behaved similarly, except that their velocity fluctuations were larger. After rising several bubble diameters, the nearly uniform distribution transitioned to a completely different state where the bubbles accumulate in vertical streams, rising much faster than when they are uniformly distributed. This behavior can be explained by the dependency of the lift force that the bubbles experience on the deformation of the bubbles. If a large number of bubbles clump together, they look like a large bubble to the surrounding fluid and the group will rise faster than a single bubble, drawing fluid with them. A spherical bubble rising in the shear flow at the edge of this plume will experience a lift force directed out from the plume. The lift force on a deformable bubble, on the other hand, is directed into the plume as explained by Ervin and Tryggvason (1997). Spherical bubbles, temporarily crowded together, will therefore disperse, but deformable bubbles will be drawn into the plume, further strengthening it. Bunner and Tryggvason (2003) only observed streaming for relatively high void fractions but speculated that the phenomenon could best be described as a nonlinear instability that required finite size perturbation in the bubble distribution to trigger it. At low void fraction the probability of sufficiently large perturbation was small and they suggested that their simulations for lower void fractions simply had not been conducted for long enough time. To test this hypothesis, they examined the evolution of bubbles initially placed in a single column. As expected, the spherical bubbles immediately dispersed, but the deformable bubbles stayed in the column.

Although the simulations described above suggest that we are rapidly gaining considerable understanding of homogeneous bubbly flow when the Reynolds number is relatively low, in many practical situations the Reynolds number is considerably higher and it is well known that bubbles at high enough Reynolds number rise unsteadily, either wobbling as they rise or rising along a spiral path. Recent experimental studies by Ellingsen and Risso (2001) suggest that the wobbling mode may be a transitionary phase and that wobbly bubbles would eventually rise along spiral paths, if one waited long enough. Computationally

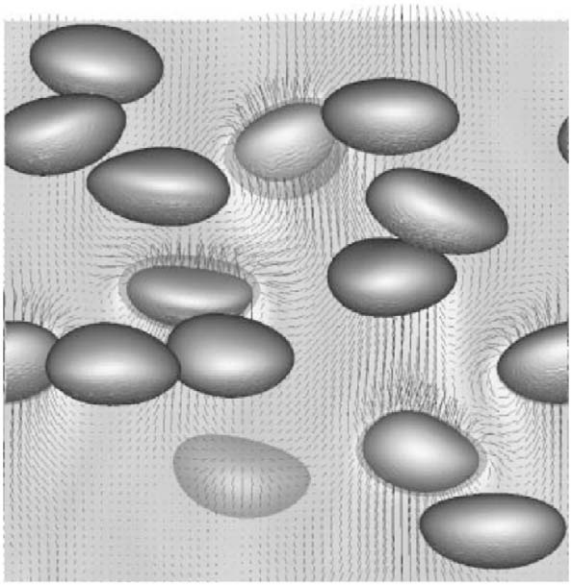

Fig. 3. One frame from a simulation of 14 wobbly bubbles in a fully periodic domain. The average rise Reynolds number is about 75 and the domain is resolved by a 128^3 grid. The bubbles and the velocity (short line segments) are shown in a plane cutting through the middle of the domain.

it is found that two-dimensional bubbles in periodic domains start to wobble at much lower rise Reynolds number than their three-dimensional counterparts. Esmaeeli et al. (1994) briefly examined bubbles that settle down into periodic wobbling and showed that the bubbles slow down significantly once they start to wobble. Göz et al. (2000) examined bubbles at higher Reynolds numbers and found what looked like a chaotic motion at high enough Reynolds numbers. They suggested that the results indicated that real (three-dimensional) deformable bubbles rising at high enough Reynolds number would exhibit chaotic motion. However, since air bubbles become spherical cap bubbles when their size (and rise Reynolds number) increases, such motion might not be observed under normal conditions.

We are currently examining the buoyancy driven motion of many bubbles at high enough Reynolds numbers so that moderately deformable bubbles show wobbly motion. Fig. 3 shows one frame from a simulation of 14 bubbles at about 6% void fraction, done using a 128^3 grid. The Eötvös number is $Eo = \rho_f g d_e^2/\sigma = 4$ and the Morton number is $M = g\mu_f^4/\rho_f\sigma^3 = 10^{-6}$, giving a rise Reynolds number of about 75. Here, the subscript f refers to the fluid. The bubbles and the fluid velocity in a plane cutting through the middle of the domain are shown at a relatively late time. Initially, the bubbles are placed randomly in a fully periodic domain but as they rise, they interact freely. While the bubbles occasionally clump together, on the average they remain essentially uniformly distributed. Given the streaming state for deformable bubbles found by Bunner and Tryggvason (2003), it is natural to ask whether wobbly bubbles stream. Since the streaming is sensitively dependent on the lift force and preliminary results for two-dimensional bubbles by Esmaeeli (1995) showed that a wobbly bubbles exhibited essentially no drift in a linear shear, it is not obvious at all that wobbly bubbles will stream. This is, indeed, what is found. Wobbly bubbles initially put in a column (in a similar way as Bunner and Tryggvason, 2003, did) immediately disperse as spherical bubbles do. Thus, examining the properties of homogeneous distribution of wobbly

bubbles is of relevance for realistic systems. Wobbly bubbles generally rise considerably slower than their non-wobbly counterpart and the velocity fluctuations are generally much larger. We note that deformation promotes unsteady rise and that air bubbles in water generally do not start to wobble until the rise Reynolds number is considerably higher. Further studies of wobbly bubbles and the effect of Reynolds number on the behavior of rising bubbles are in progress.

5. Bubbles in channels

While studies of homogeneous bubbly flows can yield considerable insight into many aspects of the interactions between freely rising bubbles, there are obviously many aspects of realistic flows that depend critically on the presence of walls. The pipe flow experiments of Serizawa et al. (1975a,b) showed, for example, increase in the concentration of bubbles near the walls in upflow in a vertical pipe. It is easy to see why nearly spherical bubbles rising in a vertical channel with upflow move toward the walls. The bubbles generally move faster than the liquid and in a shear flow the lift force on a spherical bubble is directed toward the slower moving fluid. In this case the slower moving fluid is near the wall and the bubble is therefore pushed toward it. For down-flow, the same arguments suggest that the bubbles move away from walls, as seen experimentally (Oshinowo and Charles, 1974; Wang et al., 1987). When the bubbles are very close to the wall, however, the fluid between the bubble and the wall results in a lubrication force that repels the bubble. Furthermore, as demonstrated by Ervin and Tryggvason (1997) and others, bubble deformation can result in a circulation around the bubble of the opposite sign to the fluid shear near the walls, and this results in a lift force away from the wall. The motion of bubbles near walls continues to be a topic of considerable interest as shown by the recent experimental study of de Vries et al. (2004) who studied how the trajectories of bubbles near walls change with the bubble size.

A few simulations of fully three-dimensional bubbles in a vertical channel with upflow were done by Bunner (2000) and we have recently returned to examine this problem in more details. Fig. 4 shows results

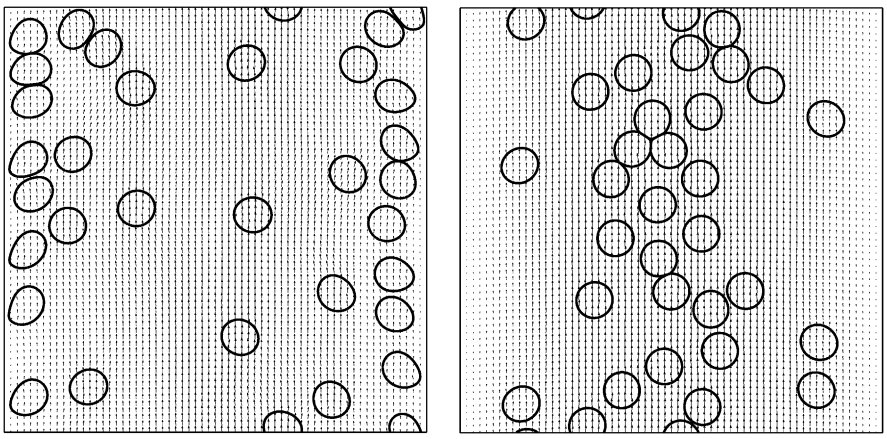

Fig. 4. The bubbles and the velocity field at a late time from two simulations of bubbles in an upward moving channel flow. In the left frame gravity is non-zero and the bubbles rise relative to the liquid, resulting in an accumulation of bubbles near the walls. In the frame on the right gravity is zero and the bubbles move with the liquid, accumulating in the center.

from two preliminary simulations of two-dimensional systems, at a relatively late stage. For both systems the initial channel Reynolds number is about thousand, the systems contain 32 bubbles of diameter less than one-tenth of the channel width, in a domain bounded by walls in the horizontal direction and periodic in the vertical direction. The surface tension is selected such that the bubbles remain nearly spherical, except in the high shear regions near the walls. For the system on the right, gravity is zero, but on the left the bubbles are buoyant and move upward relative to the liquid. It is clear that the phase distribution is very different, as expected. On the right, where the bubbles move with a velocity relatively close to the liquid velocity, they collect near the center of the channel. On the left, where the bubbles move faster than the liquid, while remaining nearly spherical except very close to the walls, the bubbles experience a lift force that pushes them out from the core, towards the walls. The wall layer does, however, lead to a relatively uniform velocity in the middle of the channel and the few bubbles left in the middle are now subject to a smaller shear and thus smaller lift. We therefore expect to see a few bubbles remaining in the core. Laminar bubbly flows have been examined experimentally by Nakoryakov et al. (1996) and Antal et al. (1991) have developed and used a two-fluid model to analyze such flows. The model showed good agreement with the experimental data, but as the results in Fig. 3 show, relatively moderate changes in the setup can lead to dramatic changes in the phase distribution. Thus, the availability of fully resolved results for three-dimensional systems should allow a very detailed comparison with available models and a thorough study of the importance of each term. The comparison of DNS results with predictions of a two-fluid model for laminar, two-dimensional bubble flow is discussed in more detail in Biswas et al. (2005).

So far, essentially all of our studies of bubbly flows have focused on relatively viscous liquids where the flow is laminar or at least would be laminar in the absence of the bubbles. Yet, multiphase flows in practical applications are often turbulent. DNS, where the continuum length and time scales of turbulent flows are fully resolved, are over 20 years old, and while DNS is limited to modest Reynolds numbers, such simulations have yielded fundamentally new insight into the structure and behavior of turbulent flows. The potential for a vastly improved understanding of turbulent bubbly flows therefore clearly exists. Indeed, many authors have examined the behavior of turbulent multiphase flow in the limit where the size of the disperse particles is small compared with smallest flow scales, and the bubbles can be represented by a point particle (see, for example, Squires and Eaton, 1990). Although the interactions between the flow and the particle are modeled and not resolved, it is likely that the results are representative of the real behavior of very small particles. For bubbles with diameters of order of a millimeter, the fundamental assumption of this approach fails and it is necessary to resolve fully the flow around each bubble, along with the turbulent flow.

We are currently conducting simulations of bubbles injected near the walls in a turbulent channel flow. The goal of this investigation is to cast some light on the mechanisms underlying drag reduction and to provide data that may be useful for the modeling of such flows. Experimental studies (see Merkle and Deutsch, 1990; Kato et al., 1995; Kodama et al., 2003 for a review) show that the injection of a relatively small amount of bubbles into a turbulent boundary layer can result in a significant reduction of the wall drag. While the general believe seems to be that the bubbles should be as small as possible (a few wall units in diameter), drag reduction is found experimentally in situations where the bubbles are considerably larger (order of 100 wall units). Fig. 5 shows one frame from a simulation of 16 bubbles in the so-called "minimum turbulent channel" of Jiménez and Moin (1991). The dimensions of the channel are $\pi \times \pi/2 \times 2$ units in the streamwise, spanwise, and wall normal direction, respectively. The channel is bounded by walls at the top and bottom and has periodic spanwise and streamwise boundaries. The wall

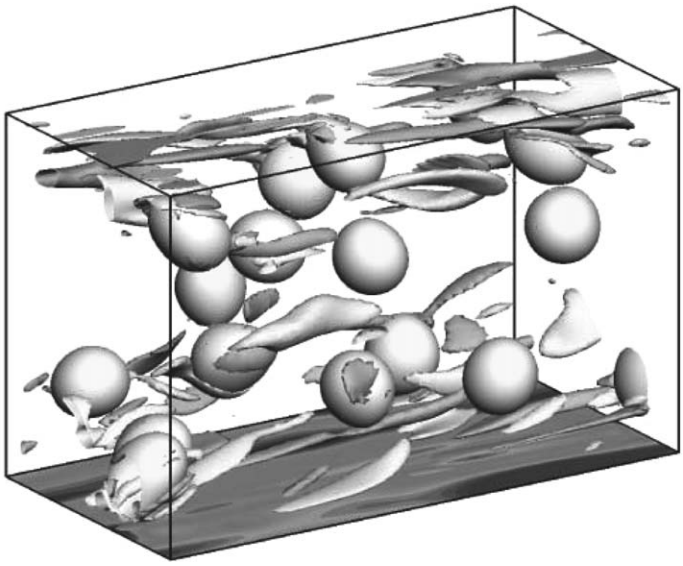

Fig. 5. One frame from a simulation of 16 bubbles in the "minimum turbulent channel." The flow is from left to right. In addition to the bubbles, iso-contours of streamwise vorticity are shown. The vorticity forms elongated structures near the walls. Dark and light shades indicate opposite signed vorticity. On the bottom, the wall shear stress is shown. Dark regions show high shear stress.

Reynolds number is $Re^+ = \rho u^+ h/\mu = 135$. Here, h is the half-height of the channel and $u^+ = \sqrt{\tau_w/\rho}$ is the friction velocity based on the average wall shear τ_w without bubbles. The computations were done using a grid of $256 \times 128 \times 192$ points, uniformly spaced in the streamwise and the spanwise direction but unevenly spaced in the wall normal direction. The initial velocity field was taken from spectral simulations of turbulent channel flows to avoid having to simulate the transition, and the volume flux is kept constant by adjusting the pressure gradient. The turbulent flow was first evolved without bubbles to ensure that the finite volume method used here correctly simulated the single-phase flow. In addition to the bubbles, isocontours of spanwise vorticity are also shown in the figure, with different shading indicating positive and negative vorticity. The results show that slightly deformable bubbles can lead to significant reduction of the wall drag by sliding over streamwise vortices and forcing them toward the wall where they are cancelled by the wall-bounded vorticity of the opposite sign. Spherical bubbles, on the other hand, often reach into the viscous sublayer where they are slowed down and lead to a large increase in drag. For more details, see Lu et al. (2005). For other work on bubbles in a turbulent channel see Kanai and Miyata (2001) and Kawamura and Kodama (2002). Neither simulation did, however, show drag reduction.

6. Formation of bubbles

In essentially all DNS of dispersed bubbly flows it has been assumed that the bubbles already exist at the start of the simulation. Yet, in reality the bubbles must be injected into the flow or be generated in some other way. In many cases the bubbles are formed as air is injected through a hole in

a wall or a needle sticking into the flow domain. The injection through a nozzle flush with the wall has been simulated by Takahira and Banerjee (2004) who used a level set method to simulate the injection of air into a shear flow and the subsequent formation of a bubble. By solving for the flow in the nozzle, they improved on the results of an earlier study by Badalassi et al. (2000) where the bubble growth was simulated but no detachment from the wall was seen. Simulations of the injection of air through a needle, assuming inviscid flow and using a boundary integral method has been done by Oguz and Prosperetti (1993).

Bubbles are also generated by degassing of the liquid or by evaporation, either due to a drop in pressure (cavitation) or rise in temperature (boiling). While several authors have examined the behavior of cavitation bubbles numerically (see, for example, Blake and Gibson, 1987, for an early review), usually using simplified models for the phase change, computations of the formation of bubbles by boiling are more recent. We have extended the method described in Section 2 to boiling flows (Juric and Tryggvason, 1998; Esmaeeli and Tryggvason, 2003) and used it to examine a number of problems. Those include explosive boiling of a nucleus in an initially superheated liquid (Esmaeeli and Tryggvason, 2003) and film boiling on a flat plate (Esmaeeli and Tryggvason, 2004a,b). For the film boiling we examined, in particular, how large systems, where bubbles broke off from the vapor film at the wall, differed from systems where the bubble growth was forced to take place at the linearly most unstable wavelength. The main question was whether subharmonic instabilities would lead to competition between waves and the formation of larger bubbles. Such meargers are seen in many other systems, but here we found that such competition was relatively weak. For an interface perturbed by the most unstable wave a mearger would occasionally take place, but the freely evolving system generally formed bubbles from sites separated by a distance slightly longer than the most unstable wavelength and in those cases mergers were very rare. Simulations with only one wave therefore generally resulted in heat transfer rates in good agreement with larger systems. We also examined the effect of the wall superheat on the boiling of a finite depth pool. For low wall superheat (but high enough to prevent wetting and a transition to nucleate boiling) bubbles broke away from the vapor film. At higher superheat the vapor production was sufficiently fast so that long vapor vents formed, sometimes reaching the surface of the pool. At even higher superheat the vents became unsteady, resulting in unsteady churn-like boiling. For moderate superheat where the vapor dynamics was much faster than the total evaporation rate of the pool, the system reached a well-defined steady state, but at high superheat all the liquid quickly evaporated and no steady state emerged. Other recent numerical studies of boiling on a flat wall include Son and Dhir (1998), Welch and Wilson (2000), Shin and Juric (2002), Yoon et al. (2001), Kunugi (2001), and Son et al. (2002).

We have also recently started to study film boiling from one or more circular tubes. Since a heated wire or a rod is a common component in practical situations, a number of experimentalists have examined this problem (Pomerantz, 1964; Lienhard and Sun, 1970). The ratio of the diameter of the wire to the capillary length scale defines limiting cases. When this ratio is very small, in particular, we expect the vapor layer to grow initially cylindrically, independent of the diameter of the cylinder. Fig. 6 shows three frames from a simulation of vapor production from a heated cylinder, immersed in a liquid pool. Gravity acts downward and the liquid pool is capped by a vapor region, open to the outside. Initially, the cylinder is surrounded by a vapor film whose radius is perturbed by a wave of the most-unstable capillary length. As the hot cylinder produces additional vapor and buoyancy lifts the vapor upward, a bubble is formed. Preliminary results indicate that the numerical predictions agree with experimental results for moderate sized cylinders. For more details see Esmaeeli and Tryggvason (2004c).

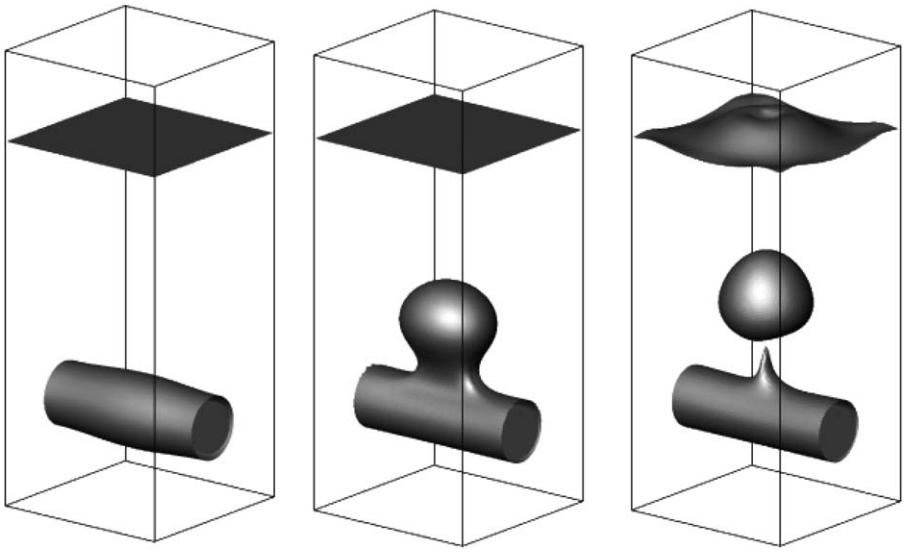

Fig. 6. Simulation of the generation of vapor bubbles from a hot cylinder immersed in a liquid pool with a vapor on the top. The phase boundary is shown at three times. In the first frame (left) a cylindrical vapor film encloses the solid cylinder. In the second frame (middle) the vapor region has grown and risen by buoyancy. In the last frame (right) one bubble has coalesced with the top surface and another bubble has broken away from the cylinder.

7. Conclusion

Direct numerical simulations of disperse bubbly flows have come a long way during the last decade. It is now possible to follow the motion of hundreds of bubbles at finite Reynolds numbers in simple geometries for sufficiently long time so that meaningful averages can be computed. At higher Reynolds numbers, the number of grid points required to resolve each bubble and the flow around them increases and the cost of doing simulations with many bubbles becomes larger. As faster computers are developed, such simulations will become increasingly more feasible. The formation of bubbles, as well as coalescence must also be addressed and except for a few simulations of the breakup of drops in well-defined flows, little has been done yet. These problems are, nevertheless, well within reach.

In many cases, gas/liquid flows cannot be modeled as disperse flows and it is necessary to resort to more complex models. In turbulent churn flows, intermixed regions of gas and liquid undergoing continuous breakup and coalescence must be modeled, and even for relatively simple stratified and annular flows, wave breaking, droplet formation and bubble entrainment must be accounted for. Additional physics, such as evaporation or surfactants adds further complications. Thus, it seems safe to conclude that much remains to be done before direct numerical simulations of multiphase flows become routine. Furthermore, as direct numerical simulations of multiphase flows become more common, the need for advances in the development of the theoretical framework for modeling such flows is also becoming more urgent. Current models were mostly developed in an environment where relatively little was known about the details of the flow, and for the most part these models are far behind what is available for single-phase turbulent flows. While our abilities to simulate directly more and more complex multiphase systems will certainly increase dramatically in the next few years, it is important to realize that our desire to compute will always

be ahead of what we can do by direct numerical simulations. Even if we could fully compute the behavior of a particular system, we can easily imagine, for example, that we might want to incorporate simulations into a real-time control algorithm that dynamically explores the consequences of several possible control actions. Thus, the condensation of knowledge obtained by direct numerical simulations into reduced or averaged models that allow faster predictions will remain at the core of multiphase flow research for a long time to come.

Acknowledgments

Most recently, our work on bubbles at high Reynolds numbers, drag reduction, and boiling, has been supported by DOE, DARPA, and NASA, respectively. Earlier support by NSF and ONR is also acknowledged.

References

Anderson, D.M., McFadden, G.B., Wheeler, A.A., 1998. Diffuse-interface methods in fluid mechanics. Ann. Rev. Fluid Mech. 30, 139–165.

Antal, S.P., Lahey, R.T., Flaherty, J.E., 1991. Analysis of phase distribution in fully developed laminar bubbly two-phase flows. Int. J. Multiphase Flow 15, 635–652.

Badalassi, V., Takahira, H., Banerjee, S., 2000. Numerical simulation of three dimensional bubble growth and detachment in a microgravity shear flow. In: Proceedings of the Fifth Microgravity Fluid Physics and Transport Phenomena Conference, NASA Glenn Research Center, Cleveland, OH, CP-2000-210470, pp. 912–914.

Baker, G.R., Meiron, D.I., Orszag, S.A, 1980. Vortex simulation of the Rayleigh–Taylor instability. Phys. Fluids 23, 1485–1490.

Baker, G.R., Meiron, D.I., Orszag, S.A., 1982. Generalized vortex methods for free surface flows problems. J. Fluid Mech. 123, 477.

Biswas, S., Esmaeeli, A., Tryggvason, G., 2005. Comparison of results from DNS of bubbly flows with a two-fluid model for two-dimensional laminar flows. Int. J. Multiphase Flow, 31, 1036–1048.

Blake, J.R., Gibson, D.C., 1981. Growth and collapse of a vapour cavity near a free surface. J. Fluid Mech. 111, 123–140.

Blake, J.R., Gibson, D.C., 1987. Cavitation bubbles near boundaries. Ann. Rev. Fluid Mech. 19, 99–123.

Boulton-Stone, J.M., Blake, J.R., 1993. Gas-bubbles bursting at a free-surface. J. Fluid Mech. 254, 437–466.

Brady, J.F., Bossis, G., 1988. Stokesian dynamics. Ann. Rev. Fluid Mech. 20, 111–157.

Bunner, B., 2000. Numerical simulations of gas–liquid bubbly flows. Ph.D. Thesis, The University of Michigan.

Bunner, B., Tryggvason, G., 1999. Direct numerical simulations of three-dimensional bubbly flows. Phys. Fluids 11, 1967–1969.

Bunner, B., Tryggvason, G., 2002a. Dynamics of homogeneous bubbly flows: part 1. Rise velocity and microstructure of the bubbles. J. Fluid Mech. 466, 17–52.

Bunner, B., Tryggvason, G., 2002b. Dynamics of homogeneous bubbly flows. Part 2, fluctuations of the bubbles and the liquid. J. Fluid Mech. 466, 53–84.

Bunner, B., Tryggvason, G., 2003. Effect of bubble deformation on the stability and properties of bubbly flows. J. Fluid Mech. 495, 77–118.

Chahine, G.L., Duraiswami, R., 1992. Dynamic interactions in a multibubble cloud. ASME J. Fluids Eng. 114 (4), 680–686.

Chan, R.K.-C, Street, R.L., 1970. A computer study of finite-amplitude water waves. J. Comput. Phys. 6, 68–94.

Chapman, R.B., Plesset, M.S., 1972. Nonlinear effects in the collaps of a nearly spherical cavity in a liquid. Trans. ASME J. Basic Eng. 94, 142.

Choi, H.G., Joseph, D.D., 2001. Fluidization by lift of 300 circular particles in plane Poiseuille flow by direct numerical simulation. J. Fluid Mech. 438, 101–128.

Daly, B.J., 1969a. Numerical study of the effect of surface tension on interface instability. Phys. Fluids 12, 1340–1354.

Daly, B.J., 1969b. A technique for including surface tension effects in hydrodynamic calculations. J. Comput. Phys. 4, 97–117.

Daly, B.J., Pracht, W.E., 1968. Numerical study of density-current surges. Phys. Fluids 11, 15–30.

de Vries, A.W.G., Biesheuvel, A., van Wijngaarden, L., 2004. Notes on the path and wake of a gas bubble rising in pure water. Int. J. Multiphase Flow 28, 1823–1835.

Drew, D.A., 1983. Mathematical modeling of two-phase flow. Ann. Rev. Fluid Mech. 15, 261–291.

Drew, D.A., Lahey Jr., R.T., 1993. Analytical modeling of multiphase flow. In: Roco, M.C. (Ed.), Particulate Two-phase Flow. Butterworth-Heinemann, Boston.

Druzhinin, O.A., Elghobashi, S.E., 2001. Direct numerical simulation of a three-dimensional spatially-developing bubble-laden mixing layer with two-way coupling. J. Fluid Mech. 429, 23–61.

Ellingsen, K., Risso, F., 2001. On the rise of an ellipsoidal bubble in water: oscillatory paths and liquid-induced velocity. J. Fluid Mech. 440, 235–268.

Ervin, E.A., Tryggvason, G., 1997. The rise of bubbles in a vertical shear flow. ASME J. Fluid Eng. 119, 443–449.

Esmaeeli, A., 1995. Numerical simulations of bubbly flows. Ph.D. Thesis, The University of Michigan.

Esmaeeli, A., Tryggvason, G., 1996. An inverse energy cascade in two-dimensional, low Reynolds number bubbly flows. J. Fluid Mech. 314, 315–330.

Esmaeeli, A., Tryggvason, G., 1998. Direct numerical simulations of bubbly flows. Part I—Low Reynolds number arrays. J. Fluid Mech. 377, 313–345.

Esmaeeli, A., Tryggvason, G., 1999. Direct numerical simulations of bubbly flows. Part II—Moderate Reynolds number arrays. J. Fluid Mech. 385, 325–358.

Esmaeeli, A., Tryggvason, G., 2003. Computations of explosive boiling in microgravity. J. Sci. Comput. 19, 163–182.

Esmaeeli, A., Tryggvason, G., 2004a. Computations of multimode film boiling on horizontal surfaces. Part I. Int. J. Heat Mass Transfer 47, 5451–5461.

Esmaeeli, A., Tryggvason, G., 2004b. Computations of multimode film boiling on horizontal surfaces. Part II. Int. J. Heat Mass Transfer 47, 5463–5476.

Esmaeeli, A., Tryggvason, G., 2004c. A front tracking method for computations of boiling in complex geometries. Int. J. Multiphase Flow 30, 1037–1050.

Esmaeeli, A., Ervin, E., Tryggvason, G., 1994. Numerical simulations of rising bubbles. In: Blake, J.R., Boulton-Stone, J.M., Thomas, N.H. (Eds.), Bubble Dynamics and Interface Phenomena. Kluwer, Dordrecht, pp. 247–255.

Fedkiw, R., Aslam, T., Merriman, B., Osher, S., 1999. A non-oscillatory Eulerian approach to interfaces in multimaterial flows (the ghost fluid method). J. Comput. Phys. 152, 457–492.

Feng, J., Hu, H.H., Joseph, D.D., 1994. Direct simulation of initial value problems for the motion of solid bodies in a Newtonian fluid, part 1. Sedimation. J. Fluid Mech. 261, 95–134.

Feng, J., Hu, H.H., Joseph, D.D., 1995. Direct simulation of initial value problems for the motion of solid bodies in a Newtonian fluid, part 2. Couette and Poiseuilli flows. J. Fluid Mech. 277, 271–301.

Floryan, J.M., Rasmussen, H., 1989. Numerical analysis of viscous flows with free surfaces. Appl. Mech. Rev. 42, 323–341.

Foote, G.B., 1973. A numerical method for studying liquid drop behavior: simple oscillations. J. Comput. Phys. 11, 507–530.

Foote, G.B., 1975. The water drop rebound problem: dynamics of collision. J. Atmos. Sci. 32, 390–402.

Fortes, A., Joseph, D.D., Lundgren, T., 1987. Nonlinear mechanics of fluidization of beds of spherical particles. J. Fluid Mech. 177, 467–483.

Fukai, J., Shiiba, Y., Yamamoto, T., Miyatake, O., Poulikakos, D., Megaridis, C.M., Zhao, Z., 1995. Wetting effects on the spreading of a liquid droplet colliding with a flat surface: experiment and modeling. Phys. Fluids 7, 236–247.

Glimm, J., McBryan, O., 1985. A computational model for interfaces. Adv. Appl. Math. 6, 422–435.

Glowinski, R., Pan, T.W., Helsa, T.I., Joseph, D.D., Periaux, J., 2001. A fictitious domain approach to the direct numerical simulation of incompressible viscous flow past moving rigid bodies: application to particulate flow. J. Comput. Phys. 169, 363–426.

Göz, M.F., Bunner, B., Sommerfeld, M., Tryggvason, G., 2000. FEDSM2000-11151: the unsteady dynamics of two-dimensional bubbles in a regular array. In: Proceedings of the ASME FEDSM00 Fluids Engineering Division Summer Meeting, June 11–15, 2000, Boston, MA.

Harlow, F.H., Welch, J.E., 1965. Numerical calculation of time-dependent viscous incompressible flow of fluid with a free surface. Phys. Fluid 8, 2182–2189.

Harlow, F.H., Welch, J.E., 1966. Numerical study of large-amplitude free-surface motions. Phys. Fluid 9, 842–851.

Harper, J.F., 1997. Bubbles rising in line: why is the first approximation so bad? J. Fluid Mech. 351, 289–300.

Hirt, C.W., Nichols, B.D., 1981. Volume of fluid (VOF) method for the dynamics of free boundaries. J. Comput. Phys. 39, 201–226.

Hirt, C.W., Cook, J.L., Butler, T.D., 1970. A Lagrangian method for calculating the dynamics of an incompressible fluid with a free surface. J. Comput. Phys. 5, 103–124.
Hou, T.Y., Lowengrub, J.S., Shelley, M.J., 2001. Boundary integral methods for multicomponent fluids and multiphase materials. J. Comput. Phys. 169, 302–362.
Hu, H.H., 1996. Direct simulation of flows of solid–liquid mixtures. Int. J. Multiphase Flow 22, 335–352.
Hu, H.H., Patankar, N.A., Zhu, M.Y., 2001. Direct numerical simulations of fluid–solid systems using Arbitrary-Lagrangian–Eularian techniques. J. Comput. Phys. 169, 427–462.
Hyman, J.M., 1984. Numerical methods for tracking interfaces. Physica D 12, 396–407.
Ishii, M., 1987. Interfacial Area Modeling. Multiphase Science and Technology 3, 31–61.
Jiménez, J., Moin, P., 1991. The minimal flow unit in near-wall turbulence. J. Fluid. Mech. 225, 213–240.
Johnson, A.A., Tezduyar, T.E., 1997. 3D simulation of fluid–particle interactions with the number of particles reaching 100. Comput. Methods Appl. Mech. Eng. 145, 301–321.
Juric, D., Tryggvason, G., 1998. Computations of boiling flows. Int. J. Multiphase Flow 24, 387–410.
Kanai, A., Miyata, H., 2001. Direct numerical simulation of wall turbulent flows with microbubbles. Int. J. Numer. Methods Fluids 35, 593–615.
Kato, H., Miyanaga, M., Yamaguchi, H., Guin, M.M., 1995. Frictional drag reduction by injecting bubbly water into turbulent boundary layer and the effect of plate orientation. In: Proceedings of the Second International Conference on Multiphase Flow 95, ICMF95, pp. 31–38.
Kawamura, T., Kodama, Y., 2002. Numerical simulation method to resolve interactions between bubbles and turbulence. Int. J. Heat Fluid Flow 23, 627–638.
Kodama, Y., Kakugawa, A., Takahashi, T., Nagaya, S., Sugiyama, K., 2003. Microbubbles: drag reduction and applicability to ships. In: Twenty-Fourth Symposium on Naval Hydrodynamics, Naval Studies Board (NSB). Available at: ⟨http://books.nap.edu/books/NI000511/html/⟩.
Kunugi, T., 2001. Mars for multiphase calculation. Comput. Fluid Dynamics J. 9, 563–571.
Ladd, A.J.C., 1993. Dynamical simulations of sedimenting spheres. Phys. Fluids A 5, 299–310.
Lee, L., LeVeque, R.J., 2003. An immersed interface method for incompressible Navier–Stokes equations. SIAM J. Sci. Comput. 25, 832–856.
LeVeque, R.J., 2002. Finite Volume Methods for Hyperbolic Problems. Cambridge University Press, Cambridge.
Lienhard, J.H., Sun, K.-H., 1970. Effect of gravity and size upon film boiling from horizontal cylinders. J. Heat Transfer 92, 292–298.
Loewenberg, M., Hinch, E.J., 1996. Numerical simulation of a concentrated emulsion in shear flow. J. Fluid Mech. 321, 395–419.
Longuet-Higgins, M.S., Cokelet, E.D., 1976. The deformation of steep surface waves on water. I. A numerical method of computation. Proc. R. Soc. London Ser. A 350, 1–36.
Lu, J., Fernández, A., Tryggvason, G., 2005. The effect of bubbles on the wall-drag in a turbulent channel flow. Phys. Fluids 17, 095102.
Merkle, C.L., Deutsch, S., 1990. Drag reduction in liquid boundary layers by gas injection. Prog. Astronaut. Aeronaut. 123, 351–412.
Michaelides, E.E., 2003. Hydrodynamic force and heat/mass transfer from particles, bubbles, and drops the Freeman scholar lecture. J. Fluids Eng. 125, 209–238.
Mitchell, T.M., Hammitt, F.H., 1973. Asymmetric cavitation bubble collapse. Trans. ASME J. Fluids Eng. 95, 29.
Nakoryakov, V.E., Kashinsky, O.N., Randin, V.V., Timkin, L.S., 1996. Gas–liquid bubbly flow in vertical pipes. J. Fluids Eng. 118, 377–382.
Oguz, H., Prosperetti, A., 1990. Bubble entrainment by the impact of drops on liquid surfaces. J. Fluid Mech. 219, 143–179.
Oguz, H., Prosperetti, A., 1993. Dynamics of bubble growth and detachment from a needle. J. Fluid Mech. 257, 111–145.
Oran, E.S., Boris, J.P., 1987. Numerical Simulation of Reactive Flow. Elsevier, Amsterdam.
Osher, S., Fedkiw, R.P., 2001. Level set methods. J. Comput. Phys. 169, 462–502.
Oshinowo, T., Charles, M.E., 1974. Vertical two-phase flow, part 1. Flow pattern correlations. Can. J. Chem. Eng. 52, 25–35.
Pan, T.W., Joseph, D.D., Bai, R., Glowinski, R., Sarin, V., 2002. Fluidization of 1204 spheres: simulation and experiment. J. Fluid Mech. 451, 169–191.
Pan, Y., Banerjee, S., 1997. Numerical investigation of the effects of large particles on wall-turbulence. Phys. Fluids 9, 3786–3807.

Pomerantz, M.L., 1964. Film boiling on a horizontal tube in increased gravity fields. Trans. ASME 86, 213–219.
Pozrikidis, C., 1992. Integral and Singularity Methods for Linearized Viscous Flow. Cambridge University Press, Cambridge.
Pozrikidis, C., 2001. Interfacial dynamics for Stokes flow. J. Comput. Phys. 169, 250–301.
Rallison, J.M., Acrivos, A., 1978. A numerical study of the deformation and burst of as viscous drop in an extensional flow. J. Eng. Mech. 89, 191.
Robinson, P.B., Blake, J.R., Kodama, T., Shima, A., Tomita, Y., 2001. Interaction of cavitation bubbles with a free surface. J. Appl. Phys. 89, 8225–8237.
Ryskin, G., Leal, L.G., 1984. Numerical solution of free-boundary problems in fluid mechanics. Part 2. Buoyancy-driven motion of a gas bubble through a quiescent liquid. J. Fluid Mech. 148, 19–35.
Sangani, A.S., Didwania, A.K., 1993. Dynamic simulations of flows of bubbly liquids at large Reynolds numbers. J. Fluid Mech. 250, 307–337.
Sankaranarayanan, K., Shan, X., Kevrekidis, I.G., Sundaresan, S., 2002. Analysis of drag and virtual mass forces in bubbly suspensions using an implicit formulation of the lattice Boltzmann method. J. Fluid Mech. 452, 61–96.
Scardovelli, R., Zaleski, S., 1999. Direct numerical simulation of free-surface and interfacial flow. Ann. Rev. Fluid Mech. 31, 567–603.
Schultz, W.W., Huh, J., Griffin, O.M., 1994. Potential-energy in steep and breaking waves. J. Fluid Mech. 278, 201–228.
Serizawa, A., Kataoka, I., Michiyoshi, I., 1975a. Turbulence structure of air–water bubbly flow. II Local properties. Int. J. Multiphase Flow 2, 235–246.
Serizawa, A., Kataoka, I., Michiyoshi, I., 1975b. Turbulence structure of air–water bubbly flow. III Transport properties. Int. J. Multiphase Flow 2, 247–259.
Sethian, J.A., 2001. Evolution, implementation, and application of level set and fast marching methods for advancing fronts. J. Comput. Phys. 169, 503–555.
Shan, X.W., Chen, H.D., 1993. Lattice Boltzmann model for simulation flows with multiple phases and components. Phys. Rev. E 47, 1815–1819.
Shin, S., Juric, D., 2002. Modeling three-dimensional multiphase flow using a level contour reconstruction method for front tracking without connectivity. J. Comput. Phys. 180, 427–470.
Shopov, P.J., Minev, P.D., Bazhekov, I.B., Zapryanov, Z.D., 1990. Interaction of a deformable bubble with a rigid wall at moderate Reynolds numbers. J. Fluid Mech. 219, 241–271.
Shyy, W., Udaykumar, H.S., Rao, M., Smith, R., 1996. Computational Fluid Dynamics with Moving Boundaries. Taylor & Francis, Bristol, PA.
Smereka, P., 1993. On the motion of bubbles in a periodic box. J. Fluid Mech. 254, 79–112.
Son, G., Dhir, V.K., 1998. Numerical simulation of film boiling near critical pressures with a level set method. J. Heat Transfer 120, 183–192.
Son, G., Ramanujapu, N., Dhir, V.K., 2002. Numerical simulation of bubble merger process on a single nucleation site during pool nucleate boiling. ASME J. Heat Transfer 124, 51–62.
Spelt, P.D.M., Biesheuvel, A., 1997. On the motion of gas bubbles in homogeneous isotropic turbulence. J. Fluid Mech. 336, 221–244.
Squires, K.D., Eaton, J.K., 1990. Particle response and turbulence modification in isotropic turbulence. Phys. Fluids 2, 1191–1203.
Sussman, M., Smereka, P., Osher, S., 1994. A level set approach for computing solutions to incompressible two-phase flows. J. Comput. Phys. 114, 146–159.
Takada, N., Misawa, M., Tomiyama, A., Fujiwara, S., 2000. Numerical simulation of two- and three-dimensional. Two-phase fluid motion by lattice Boltzmann method. Comput. Phys. Commun. 129, 233–246.
Takada, N., Misawa, M., Tomiyama, A., Hosokawa, S., 2001. Simulation of bubble motion under gravity by lattice Boltzmann method. J. Nucl. Sci. Technol. 38, 330–341.
Takagi, S., Matsumoto, Y., Huang, H., 1997. Numerical analysis of a single rising bubble using boundary-fitted coordinate system. JSME Int. J. Ser. B 40, 42–50.
Takahira, H., Banerjee, S., 2004. Numerical analysis of three dimensional bubble growth and detachment in a shear flow. In: Proceedings of ICMF2004. International Conference on Multiphase Flow.
Tomiyama, A., Zun, I., Sou, A., Sakaguchi, T., 1993. Numerical analysis of bubble motion with the VOF method. Nucl. Eng. Design 141, 69–82.

Tryggvason, G., Bunner, B., Esmaeeli, A., Juric, D., Al-Rawahi, N., Tauber, W., Han, J., Nas, S., Jan, Y.-J, 2001. A front tracking method for the computations of multiphase flow. J. Comput. Phys. 169, 708–759.

Unverdi, S.O., Tryggvason, G., 1992a. A front-tracking method for viscous incompressible multi-fluid flows. J. Comput. Phys. 100, 25–37.

Unverdi, S.O., Tryggvason, G., 1992b. Computations of multi-fluid flows. Physica D 60, 70–83.

Vinje, T., Brevig, P., 1981. Numerical simulations of breaking waves. Adv. Water Resources 4, 77–82.

Wang, S.K., Lee, S.J., Jones Jr., O.C., Lahey Jr., R.T., 1987. 3-D turbulence structure and phase distribution in bubbly two-phase flows. Int. J. Multiphase Flow 13, 327–343.

Welch, S.W.J., Wilson, J., 2000. A volume of fluid based method for fluid flows with phase change. J. Comp. Phys. 160, 662–682.

Xu, J., Maxey, M.R., Karniadakis, G.E., 2000. Numerical simulation of turbulent drag reduction using micro-bubbles. J. Fluid Mech. 468, 271–281.

Xue, M., Xu, H.B., Liu, Y.M., Yue, D.K.P., 2001. Computations of fully nonlinear three-dimensional wave–wave and wave–body interactions. Part 1. Dynamics of steep three-dimensional waves. J. Fluid Mech. 438, 11–39.

Yabe, T., Xiao, F., Utsumi, T., 2001. The constrained interpolation profile (CIP) method for multi-phase analysis. J. Comput. Phys. 169, 556–593.

Ye, T., Mittal, R., Udaykumar, H.S., Shyy, W., 1999. An accurate Cartesian grid method for viscous incompressible flows with complex immersed boundaries. J. Comput. Phys. 156, 209–240.

Yoon, H.Y., Koshizuka, S., Oka, Y., 2001. Direct calculation of bubble growth, departure, and rise in nucleate pool boiling. Int. J. Multiphase Flow 27, 277–298.

Youngren, G.K., Acrivos, A., 1976. On the shape of a gas bubble in a viscous extensional flow. J. Fluid Mech. 76, 433.

Yu, D.G., Tryggvason, G., 1990. The free surface signature of unsteady, two-dimensional vortex flows. J. Fluid Mech. 218, 547–572.

Zhang, D.Z., Prosperetti, A., 1994. Ensemble phase-averaged equations for bubbly flows. Phys. Fluids 6, 2956–2970.

Zhou, H., Pozrikidis, C., 1993. The flow of ordered and random suspensions of two-dimensional drops in a channel. J. Fluid Mech. 255, 103–127.

Zinchenko, A.Z., Davis, R.H., 2000. An efficient algorithm for hydrodynamical interaction of many deformable drops. J. Comput. Phys. 157, 539–587.